

# Timescale Analysis for a Standard Rotating Detonation Rocket Engine

Raj T. Dave

Department of Mechanical and Aerospace Engineering, University of Alabama in Huntsville  
Huntsville, AL 35899, USA

Jason R. Burr

Rocket Combustion Devices Branch, Air Force Research Laboratory  
Edwards Air Force Base, CA 93524, USA

Mathias C. Ross

Department of Mechanical and Aerospace Engineering, University of California at Los Angeles

John. W. Bennowitz

Department of Mechanical and Aerospace Engineering, University of Alabama in Huntsville  
Huntsville, AL 35899, USA

## 1 Introduction

Rotating detonation rocket engines (RDREs) implement a new propulsion cycle that uses detonation-based combustion as the primary means of efficiently converting the chemical energy contained within the reactants to bulk thermal energy of the combustion products. Recently, there has been increased interest in detonation-based propulsion devices due to their potential advantages over traditional deflagration-based combustion cycles. In particular, detonation is a supersonic, thermally-driven shock that produces heat release at elevated pressure, which translates into a 10% theoretical maximum increase in engine thrust  $F$  and specific impulse  $I_{sp}$  [1, 2]. In addition, detonation-based propulsion devices create compact combustion zones, allowing substantial size and weight reduction. Finally, these devices are substantially less susceptible to the onset of hardware damaging thermo-acoustic instabilities, which is a common design challenge for traditional deflagration-based rocket engines [3].

In rotating detonation rocket engines, one or more detonation wave(s) travel around the annulus supersonically, which convert the injected propellants into combustion products via detonation. The existence of the traveling detonations cause additional characteristic timescale considerations apart from those associated with traditional processes in rocket chambers (e.g., flow, acoustic). Previously, certain aspects of these additional processes have been investigated for detonation-based combustors including kinetic timescale effects [4], deflagration-based timescale considerations [5], and wave stability [6]. In addition, specific characteristic timescales including detonation chemical timescales and those associated with injection recovery due to a wave passage event were assessed for a range of chamber conditions and rocket relevant propellants in a previous work by Bennowitz et al. [7]. The objective of this current effort is to expand upon this previous work by implementing the first-principle models from Bennowitz et al. to perform a case study on the 76.2 mm outer diameter (OD) standard RDRE design, which is part

of the United States Air and Space Force's detonation-based propulsion technology transition plan [8]. This will enable further understanding of the underlying physics associated with this experimentally analyzed RDRE, which will ultimately influence the development of the next generation high-performing RDRE flight demonstrator.

## 2 Engine Hardware & Flow Conditions

The rotating detonation rocket engine geometry considered in the study is modeled after a standard RDRE configuration that has been used in previous experimental and numerical studies [9, 10], which consists of a straight annular design with 76.2 mm OD, 76.2 mm length and 5.08 mm annular width (see inset image in Fig. 1(a)). A flat unlike impinging injection scheme with 72 elements is implemented in this engine, where the fuel and oxidizer have individual orifice diameters of 0.787 and 1.245 mm, respectively. Each injector pair is designed to impinge at 2.16 mm axially from the annulus centerline, and operate with steady choked flow with the exception of during a transient wave passage event.

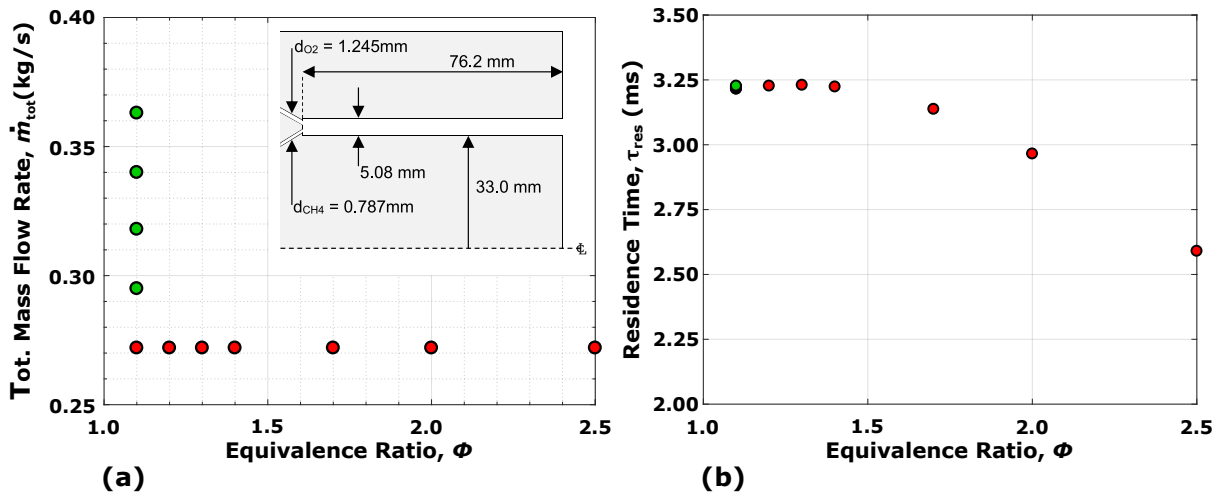


Figure 1: Investigated (a) flow conditions for the RDRE hardware, and (b) chamber residence time  $\tau_{res}$  as a function of equivalence ratio (red points) and total mass flow (green points).

Investigated flow conditions are a function of equivalence ratio  $\phi$  and total mass flow  $\dot{m}_{tot}$ , which influence detonation mode dynamics and respective timescales. Equivalence ratio drives chemistry, while  $\dot{m}_{tot}$  affects propellant fill recovery and chamber pressure. In order to investigate these effects on the characteristic timescales,  $\phi$  ranges from 1.1 to 2.5, and  $\dot{m}_{tot}$  from 0.272 to 0.363 kg/s (see Fig. 1(a)).

Reactant and product pressures in the RDRE geometry are determined analytically for each test condition. A two-variable Newton-Raphson solver is implemented to identify the combustor throat pressure and temperature that satisfy constraints of mass flux (i.e., mass flow rate per unit area), sonic flow velocity, and total enthalpy. Flow composition at the throat is assumed to be fully reacted and at equilibrium, and the local sound speed is numerically approximated through perturbations to local temperature and related to the sound speed through a series of Maxwell's thermodynamic relations. Once the throat condition is known, the total flow momentum is evaluated and used to uniquely determine the inlet state. A second two-variable Newton-Raphson solver is used to solve for combustor inlet pressure and temperature under constraints of mass flux, total momentum, and total enthalpy. At this state, the flow is solely composed of reactants, and the flow velocity represents the bulk flow of those reactants into the combustor. In addition, upstream plenum pressures are determined using choked flow analysis through

each respective injector at the prescribed condition mass flow rate for the experimentally reported injector discharge coefficients,  $C_{d,\text{fuel}}$  and  $C_{d,\text{ox}}$ . Chamber and plenum properties for three representative conditions are summarized in Table 1.

Table 1: Chamber and plenum properties for the nominal ( $\phi = 1.1$ ,  $\dot{m}_{\text{tot}} = 0.272$  kg/s), high flow ( $\phi = 1.1$ ,  $\dot{m}_{\text{tot}} = 0.363$  kg/s), and high  $\phi$  ( $\phi = 1.7$ ,  $\dot{m}_{\text{tot}} = 0.272$  kg/s) conditions.

Condition	$\phi$	$\dot{m}_{\text{tot}}$ (kg/s)	$\dot{m}_{\text{fuel}}$ (kg/s)	$\dot{m}_{\text{ox}}$ (kg/s)	$p_c$ kPa	$\frac{p_{\text{fuel}} - p_c}{p_c}$	$\frac{p_{\text{ox}} - p_c}{p_c}$	$C_{d,\text{fuel}}$	$C_{d,\text{ox}}$
Nominal	1.1	0.272	0.059	0.213	517	1.53	1.38	0.830	0.815
High Flow	1.1	0.363	0.078	0.284	692	1.42	1.33	''	''
High $\phi$	1.7	0.272	0.091	0.181	543	2.58	1.00	''	''

### 3 Flow, Acoustic and Chemical Timescales

Relevant characteristic timescales are assessed for this standard RDRE across the investigated flow conditions. Chamber residence time  $\tau_{\text{res}}$  is a foundational rocket combustor time that fixes the total available time for all the individual chamber processes to take place. Specifically, it is the time that a fluid element of propellant exists within the chamber, and is defined as  $\tau_{\text{res}} = \frac{\rho_{\text{chm}} V_{\text{chm}}}{\dot{m}_{\text{tot}}}$ , where  $\rho_{\text{chm}}$  is the combustion gas mixture density, and  $V_{\text{chm}}$  is the total combustion chamber volume.

As a function of combustion chemistry from  $\phi = 1.0$  to 2.5, residence time ranges from approximately 3.25 to 2.5 ms (see Fig. 1(b)). This is primarily due to the combustion product gas mixture density reducing as the reactant mixture becomes increasingly fuel rich. In addition,  $\tau_{\text{res}}$  is fairly insensitive while increasing the total flow rate from 0.272 to 0.363 kg/s, which is due to the fact that thermal choking of the flow exists across this entire range, causing the product mixture density to decrease in proportion to the increasing chamber mass flow. Overall, these residence times are sufficiently large to permit proper injection, mixing and detonation to occur.

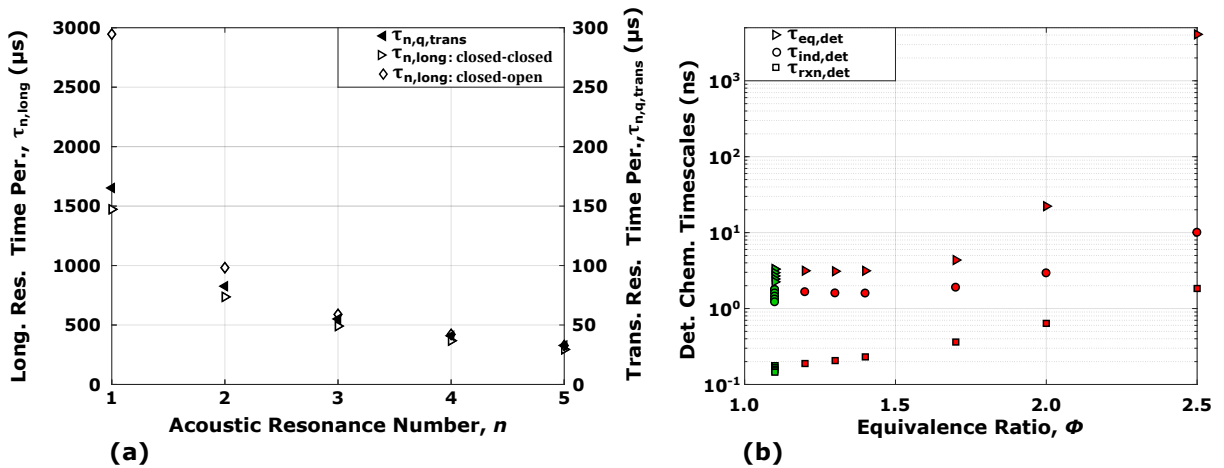


Figure 2: Timescales for the (a) longitudinal  $\tau_{n,\text{long}}$  and transverse  $\tau_{n,q,\text{trans}}$  acoustic resonances for the nominal flow condition ( $\phi = 1.1$ ,  $\dot{m}_{\text{tot}} = 0.272$  kg/s), and (b) detonation chemical times (i.e., induction  $\tau_{\text{ind,det}}$ , reaction  $\tau_{\text{rxn,det}}$ , and chemical equilibrium time  $\tau_{\text{eq,det}}$ ) for the standard RDRE.

As rotating detonation modes and spontaneous thermoacoustic instabilities observed in rockets are driven by similar underlying physics (i.e., coupling between unsteady heat release and pressure) [11], it is worthwhile to characterize the acoustic timescales associated with the annular chamber geometry.

During operation, it is possible for both longitudinal and transverse (i.e., tangential or radial) modes to become excited. Longitudinally, the RDRE has one closed acoustic boundary at the injector plate and a choked sonic plane boundary at the exit. However, as the actual chamber exhaust is oscillatory with small periodic regions of subsonic flow, longitudinal mode periods are calculated using both closed-closed and closed-open system boundaries, to fully capture this range. For a closed-closed system,  $T_{n,\text{long,cc}} = \frac{2L}{nc}$ , where  $c$  is the combustion product sound speed,  $L$  is chamber length and  $n$  is the resonance number, while for a closed-open system,  $T_{n,\text{long,co}} = \frac{4L}{(2n-1)c}$ . Additionally, transverse mode periods are found using  $T_{n,q,\text{trans}} = \frac{2\pi}{ck_{n,q}}$ , where  $k_{n,q}$  is the transverse wave number found using the approach described in Kim and Soedel [12].

Overall, the first five longitudinal modes have time periods ranging from 300 to 3000 ms for both boundary condition systems (see Fig. 2(a)). As the typical detonation mode time period for this geometry is experimentally measured to be between 45 and 65  $\mu\text{s}$ , this confirms that longitudinal coupling effects are largely separated. However, the transverse acoustic time period for the  $n = 2$  and 3 modes ranges from 83 and 55  $\mu\text{s}$ , respectively, which provides some evidence for the preferred operating mode of this RDRE to be between 2 and 3 waves for these flow conditions (which is consistent with experimental observations).

Detonation chemical timescales are found using an in-house ZND detonation solver based upon the work of Kao [13]. Three timescales are extracted from the ZND solution for each flow condition, including the induction time  $\tau_{\text{ind,det}}$ , reaction time  $\tau_{\text{rxn,det}}$  and equilibrium time  $\tau_{\text{chem,eq,det}}$ . All three characteristic chemical timescales are exponentially temperature dependent due to Arrhenius rate kinetics, therefore shortening at conditions with increased Chapman-Jouguet temperature detonations (see Fig. 2(b)). Across these conditions, maximum experimentally measured RDRE performance is observed at  $\phi = 1.1$ , which correlates to minimum values of  $\tau_{\text{ind,det}}$ ,  $\tau_{\text{rxn,det}}$  and  $\tau_{\text{chem,eq,det}}$ . Therefore, this suggests that operating at conditions which minimize chemical times largely decouples them from the other processes, and may contribute to increased overall engine performance.

#### 4 Injection Timescales

Injection recovery timescales are determined using the previous model from Bennewitz et al. [7]. This model uses a synthetically generated detonation wave profile as the primary input that is created using the ZND solution and a modified expansion profile based on the fit presented in Kaemming et al. [14] with the typical wave arrival times of 50  $\mu\text{s}$  for this RDRE. The model then determines whether the injector flow is either choked or unchoked throughout the wave profile, and if it becomes unchoked, the model can also capture combustion product back flow. If the detonation strength is sufficiently high, product back flow will occur and the amount of mass ingested is tracked and required to be expelled prior to fresh reactant injection. This permits three injection timescales to be quantified including the flow reversal time  $\tau_{\text{inj,rvs}}$ , suppression time  $\tau_{\text{inj,supp}}$  and total recovery time  $\tau_{\text{inj,rcv}}$ . Flow reversal times, i.e., the time for the back flow event to occur, average about 30  $\mu\text{s}$  for these conditions (see Fig. 3(a)). In addition, the injection suppression time, i.e., the time for reactants to inject after product plenum ingestion and expulsion, are on the order to 100  $\mu\text{s}$ , as these injectors operate at fairly low stiffness (see Table 1). This helps explain why non-idealized wave behavior is often seen in detonation-based engines, as for typical injection stiffness levels, there is not sufficient time for full recovery and mixing before the next wave passage at idealized detonation strength. Therefore, a set of weaker detonations stabilize within the chamber, which are supported by shortened injection recovery processes due to reduced product back flow and unchoking.

Summarizing the respective timescale ranges for these conditions show a few notable observations for the RDRE operation (see Fig. 3(b)). First, the chamber residence times are shown to be sufficiently long

for all of the necessary chamber processes including injection and combustion to occur. Therefore, it is possible to reduce the chamber volume by shortening the length to make it more compact for additional size/weight savings, and a timescale-based approach tailored to the propellant injection type (i.e., gas-gas, liquid-gas, liquid-liquid) can be used to appropriately size RDRE chamber lengths. Additionally, detonation chemical timescales are largely isolated from the flow, injection and acoustic timescales, which should be used as a design guideline for increased engine performance. The rest of the three timescale types including injection recovery, acoustic (in particular transverse modes) and detonation wave arrival all overlap within the same range of 10 to 100  $\mu\text{s}$ . This further illustrates the coupled nature of these devices, where the injection recovery and operating modes are inherently linked. Therefore, understanding the injection recovery process for a specific injection scheme and their relationship to the natural transverse acoustic modes of the chamber may be used as a foundation to influence the detonation operating mode.

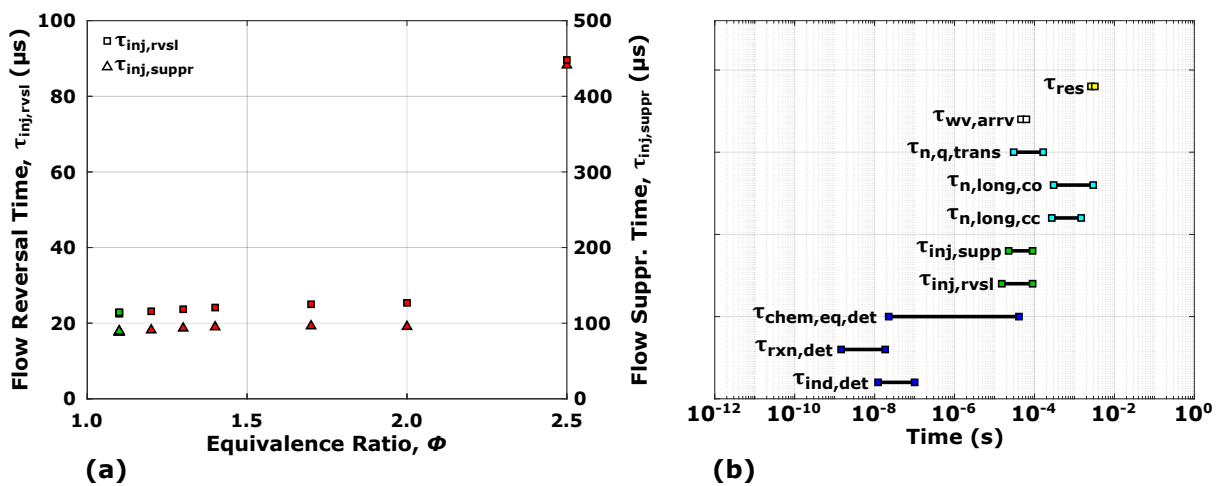


Figure 3: Injection timescales for the (a) flow reversal and suppression times, and the (b) timescale summary showing full-scale ranges of all timescales across the flow conditions.

## 5 Concluding Remarks

This study presents the relevant characteristic timescales for the standard 76.2 mm outer diameter rotating detonation rocket engine spanning various processes including chemical, injection, flow and acoustic. These timescales are determined over relevant flow conditions that have been investigated experimentally and numerically for this RDRE geometry. It is found that the typical operating mode time period values (i.e., 45 - 65  $\mu\text{s}$ ) directly overlap with that of the  $n = 2, 3$  transverse acoustic modes. Additionally, experimentally measured maximum engine performance as a function of reactant chemistry corresponds to a minimization of the detonation chemical timescales. Finally, modeled injection recovery timescales for ideal Chapman-Jouguet detonation behavior are sufficiently long ( $\approx 100 \mu\text{s}$ ), indicating why non-idealized, lower strength detonations are typically observed in non-premixed detonation-based engines.

## 6 Acknowledgments

This work has been supported by the Air Force Office of Scientific Research (AFOSR) under AFRL Lab Task 23RQCOR010 funded by the AFOSR Energy, Combustion, Non-Equilibrium Thermodynamics portfolio with Dr. Chiping Li as program manager.

---

**References**

- [1] J. R. Burr and E. Paulson, "Thermodynamic performance results for rotating detonation rocket engine with distributed heat addition using cantera," in *AIAA Propulsion and Energy 2021 Forum*. American Institute of Aeronautics and Astronautics, jul 2021. [Online]. Available: <https://doi.org/10.2514/6.2021-3682>
- [2] B. R. Bigler, E. J. Paulson, and W. A. Hargus, "Idealized efficiency calculations for rotating detonation engine rocket applications," in *53rd AIAA/SAE/ASEE Joint Propulsion Conference*. American Institute of Aeronautics and Astronautics, jul 2017. [Online]. Available: <https://doi.org/10.2514/6.2017-5011>
- [3] D. Harrje, "Liquid propellant rocket combustion instability," National Aeronautics and Space Administration, Tech. Rep., 1972.
- [4] D. P. Stechmann, S. D. Heister, and A. J. Harroun, "Rotating detonation engine performance model for rocket applications," *Journal of Spacecraft and Rockets*, vol. 56, no. 3, pp. 887–898, may 2019. [Online]. Available: <https://doi.org/10.2514/1.a34313>
- [5] R. T. Fievisohn, J. Hoke, and S. A. Schumaker, "Product recirculation and incipient autoignition in a rotating detonation engine," in *AIAA Scitech 2020 Forum*. American Institute of Aeronautics and Astronautics, jan 2020. [Online]. Available: <https://doi.org/10.2514/6.2020-2286>
- [6] P. Wolański, *Research on detonative propulsion in Poland*. Warsaw: Institute of Aviation, 2021.
- [7] J. W. Bennowitz, J. R. Burr, and C. F. Lietz, "Characteristic timescales for rotating detonation rocket engines," in *AIAA Propulsion and Energy 2021 Forum*. American Institute of Aeronautics and Astronautics, jul 2021. [Online]. Available: <https://doi.org/10.2514/6.2021-3671>
- [8] W. A. Hargus, S. A. Schumaker, and E. J. Paulson, "Air force research laboratory rotating detonation rocket engine development," in *2018 Joint Propulsion Conference*. American Institute of Aeronautics and Astronautics, jul 2018. [Online]. Available: <https://doi.org/10.2514/6.2018-4876>
- [9] J. W. Bennowitz, B. R. Bigler, M. C. Ross, S. A. Danczyk, W. A. Hargus, and R. D. Smith, "Performance of a rotating detonation rocket engine with various convergent nozzles and chamber lengths," *Energies*, vol. 14, no. 8, p. 2037, apr 2021. [Online]. Available: <https://doi.org/10.3390/en14082037>
- [10] B. R. Bigler, J. W. Bennowitz, S. A. Danczyk, and W. A. Hargus, "Rotating detonation rocket engine operability under varied pressure drop injection," *Journal of Spacecraft and Rockets*, vol. 58, no. 2, pp. 316–325, mar 2021. [Online]. Available: <https://doi.org/10.2514/1.a34763>
- [11] V. Anand and E. Gutmark, "Rotating detonation combustors and their similarities to rocket instabilities," *Progress in Energy and Combustion Science*, vol. 73, pp. 182–234, jul 2019. [Online]. Available: <https://doi.org/10.1016/j.pecs.2019.04.001>
- [12] J. Kim and W. Soedel, "General formulation of four pole parameters for three-dimensional cavities utilizing modal expansion, with special attention to the annular cylinder," *Journal of Sound and Vibration*, vol. 129, no. 2, pp. 237–254, mar 1989. [Online]. Available: [https://doi.org/10.1016/0022-460x\(889\)990580-4](https://doi.org/10.1016/0022-460x(889)990580-4)

- 
- [13] S. Kao, "Detonation stability with reversible kinetics," Ph.D. Dissertation, California Institute of Technology, 2008.
- [14] T. Kaemming, M. L. Fotia, J. Hoke, and F. Schauer, "Thermodynamic modeling of a rotating detonation engine through a reduced-order approach," *Journal of Propulsion and Power*, vol. 33, no. 5, pp. 1170–1178, sep 2017. [Online]. Available: <https://doi.org/10.2514/1.b36237>